J Therm Anal Calorim (2010) 101:49–58
DOI 10.1007/s10973-010-0852-3

Thermodynamic characteristics of a natural zinc silicate hemimorphite

Researches by the method of low-temperature adiabatic calorimetry and quantum chemical computation of vibrational states

M. R. Bissengaliyeva · N. S. Bekturganov · D. B. Gogol

RCCT2009 Special Chapter

Abstract The temperature dependence of heat capacity of a natural zinc silicate, hemimorphite $Zn_4Si_2O_7(OH)_2{\cdot}H_2O$, over the temperature range 5–320 K has been investigated by the method of low-temperature adiabatic calorimetry. On the basis of the experimental data on heat capacity over the whole temperature interval, its thermodynamic functions $C_p(T)$, $S(T)$ and $H(T) - H(0)$ have been calculated. The existence of a phase transition in the area of 90–105 K determined on the basis of vibrational spectra has been confirmed, and changes of entropy $\Delta S_{tr.}$ and enthalpy $\Delta H_{tr.}$ of the phase transition have been calculated. Hemimorphite heat capacity has also been determined by the calculation methods according to the valence force field model in LADY program. The values of force constants of valence bonds and angles have been calculated by semi-empirical method PM5. The calculated IR and Raman spectra concordant with the experimental spectra have been obtained. The heat capacity values calculated according to the found vibrational states satisfactorily agree with those experimentally obtained with an accuracy of ±1.7% in the area of 120–200 K, and not more than ±0.8% for the interval of 200–300 K. This fact testifies that the calculation of thermodynamic characteristics is correct.

Keywords Hemimorphite · Low-temperature adiabatic calorimetry · Thermodynamic functions · Quantum chemical calculation · Valence force field model

M. R. Bissengaliyeva (✉) · D. B. Gogol
Institute of Complex Development of Mineral Resources,
5, Ippodromnaya Str, Karaganda 100019, Kazakhstan
e-mail: mirabis@ipkon.kz; 160655@mail.ru

N. S. Bekturganov
JSC National Scientific-Technological Holding "Parasat",
18, Prospect Respubliki, Astana 010000, Kazakhstan

Introduction

A natural zinc silicate, hemimorphite $Zn_4Si_2O_7(OH)_2{\cdot}H_2O$, belongs to one of the most spread minerals of the oxidation zone of zinc-bearing ores, that is why it is necessary to investigate its thermodynamic properties. Geiger and Dachs [1] have researched quasi-ice-like C_p behavior of molecular H_2O in hemimorphite $Zn_4Si_2O_7(OH)_2{\cdot}H_2O$ recently. The structural features and vibration properties of this mineral have attracted the researchers' attention for quite a long time.

The crystal structure of hemimorphite has been studied in detail by the method of X-ray diffraction in the work of McDonald and Cruickshank [2], where the size of hemimorphite unit cell, the structure of tetrahedra of zinc and Si_2O_7-groups as well as the arrangement of water molecules in hemimorphite structure have been made more precise. Hill et al. [3] have investigated hemimorphite by means of the neutron diffraction method. They have determined positions of hydrogen atoms and the structure of hydrogen bonds. The system of hydrogen bonds of hemimorphite has also been investigated in the work of Takeuchi et al. [4] by the methods of X-ray and neutron diffraction. Water has been determined by these and other investigations to be present in the hemimorphite composition both in the form of H_2O molecules and in the form of hydroxyl ions. The water molecules are in the voids between coordination tetrahedra of zinc and silicon, and they are coordinated by hydrogen bonds from hydroxyl groups. The spectroscopic investigations of hemimorphite over the temperature range of 82–373 K carried out by Libowitzky and Rossman [5] proved the availability of a phase transition in the area close to 98 K. In the following work [6], the proton disordering of the specimen at low and room temperature and the absence of a phase transition

were shown by the methods of IR-spectroscopy and X-ray structure analysis of the dehydrated specimen.

Libowitzky et al. [7] investigated the low-temperature structure and the phase transition of hemimorphite and based on the neutron diffraction data, they confirmed the availability of the phase transition at 98 K, which had earlier been detected by the optical methods. The review of hemimorphite analysis by the methods of vibrational spectroscopy can be completed by the studies of Frost et al. [8] and Kolesov [9]. Thus, in their work Frost et al. investigated in detail three specimens of hemimorphite from different deposits by the methods of infrared and Raman spectroscopy at room temperature. The specimens showed identical absorption bands and the presence of bands typical for carbonate-ion in one of them. An investigation of Raman spectra of hemimorphite from the temperature of liquid helium was carried out in the work of Kolesov; and an assumption of existing one more phase transition at 20 K was made based on studying the water molecules and hydroxyl groups' vibration. Libowitzky [7] points out that some hydrogen atoms in the system of hemimorphite hydrogen bonds can be considered as atoms being in the disordered state. The lines of Raman spectra agreeable to the atoms vibration in these states are distinguished in the work of Kolesov [9], and he identifies disappearance of these lines as a phase transition.

Experimental

Description of the sample

In this work, an experimental investigation of temperature dependence of hemimorphite heat capacity over the range of 4–320 K has been carried out by the method of low-temperature adiabatic calorimetry, and theoretical computation of the mineral thermodynamical functions has also been made.

The selection of a hemimorphite monomineral fraction was performed from a sample of zinc-bearing ore from the deposit Akzhal (Kazakhstan). Hemimorphite crystals—transparent, colorless, overage size 0.2 × 0.5 × 2 mm—are represented by multiple druses (Fig. 1). The X-ray phase analysis was carried out on X-ray diffractometer DRON-3. The specimen roentgenogram corresponds to the lines of hemimorphite in the crystallographic database (Fig. 2). The specimen infrared spectrum (Fig. 3) shows the coincidence of principal absorption bands of the compound with positions of the lines given in [8].

The chemical analysis of hemimorphite has been carried out by LLP "ASITs VIMS" (Limited Liability Partnership "Analytical certification evaluation center of the All-Russian scientific-research institute of minerals named

Fig. 1 Crystals of hemimorphite (deposit Akzhal). Magnification 1000×

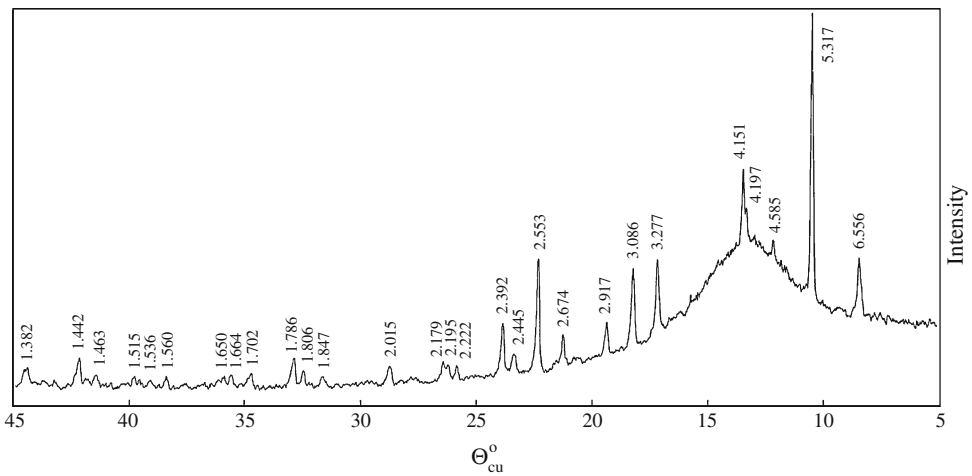

Fig. 2 An X-ray photograph of hemimorphite

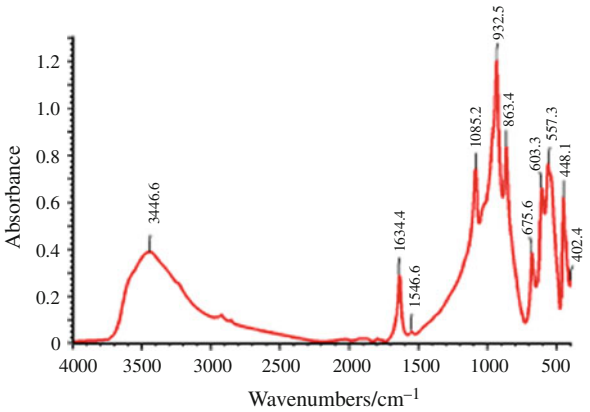

Fig. 3 The infrared spectrum of hemimorphite

after N.V. Fedorovsky"). The contents of the main elements in recalculation into oxides are as follows: zinc oxide ZnO, 69.2 mass% (determined by titrimetric method of analysis); silicon oxide SiO_2, 23.5 mass% (photometric method); bound water H_2O^+, 7.18 mass% (gravimetric method). The impurity composition of hemimorphite has been investigated by the atomic-and-absorption and mass spectrametric methods of analysis. The relative mass fraction of impurities (61 elements in total) does not exceed 0.079%. The main impurity elements are: lead Pb, 0.018%; calcium Ca, 0.016%; aluminum Al, 0.012%; sodium Na, 0.009%; and iron Fe, 0.007%.

Heat capacity measurements

The investigation experimental part has been carried out at a low-temperature thermophysical unit BKT-10.04, produced by CJSC "Termis" [10]. The unit error when measuring a standard copper specimen does not exceed ±1.43% at 5 K, ±0.75% at 10 K, ±0.23% at 40 K, ±0.075% at 90 K, ±0.060% at 120 K, ±0.068% at 200 K, ±0.091% at 270 K, and ±0.106% at 298.15 K. The temperature is measured with an iron-rhodium resistance thermometer calibrated in the VNIIFTRI (National Research Institute for Physicotechnical and Radio Engineering Measurements) in accordance with the international temperature scale ITS-90 ($R_0 = 50\ \Omega$).

A weighted portion of the specimen for analysis, being placed into a titanium container 1 cm^3 in volume, was 1.5832 g. Steps of heating were 0.3 K at 4–6 K, 0.5 K at 6–10 K, 1 K at 10–20 K, 2 K at 20–70 K and 3 K for temperatures higher than 70 K. Measurements of the heat capacity were carried out in several series: 4–35 K, 35–85 K, 80–320 K with additional series in the area of the phase transition, the value of temperature stage in the repeated measurements being of smaller value—0.5 and 0.2 K. The experimental values of hemimorphite heat capacity are presented in Table 1.

Table 1 The experimental values of hemimorphite heat capacity

T/K	C_p/J g^{-1} K^{-1}
Series 1	
4.38[a]	0.000187
4.73	0.000230
5.09	0.000294
5.34	0.000360
5.58	0.000419
5.82	0.000483
6.06	0.000550
6.39	0.000662
6.82	0.000843
7.25	0.001061
7.68	0.001311
8.12	0.001606
8.56	0.001936
9.00	0.002314
9.44	0.002736
9.89	0.003210
10.56	0.004076
11.46	0.005338
12.36	0.006754
13.27	0.008404
14.19	0.0103
15.12	0.0125
16.06	0.0146
17.01	0.0167
17.96	0.0197
18.91	0.0224
19.87	0.0252
21.32	0.0298
23.26	0.0360
25.22	0.0427
27.18	0.0498
29.16	0.0572
31.14	0.0647
33.13	0.0719
35.11	0.0803
37.09	0.0882
Series 2	
35.93	0.0834
37.99	0.0918
39.97	0.1000
41.95	0.1083
43.93	0.1164
45.92	0.1239
47.90	0.1316
49.89	0.1396
51.87	0.1483
53.86	0.1567

Table 1 continued

T/K	C_p/J g^{-1} K^{-1}
55.85	0.1640
57.84	0.1706
59.83	0.1794
61.83	0.1872
63.82	0.1947
65.82	0.2023
67.80	0.2096
69.75	0.2169
72.21	0.2263
75.22	0.2374
78.23	0.2487
81.26	0.2603
84.29	0.2729
Series 3	
79.51	0.2536
82.88	0.2668
85.93	0.2787
88.98	0.2912
92.03	0.3048
95.08	0.3206
98.12	0.3423
101.15	0.3733
104.27[a]	0.3482
107.47	0.3378
110.63	0.3442
113.75	0.3514
116.88	0.3591
120.03	0.3666
123.17	0.3742
126.33	0.3818
129.51	0.3896
132.69	0.3969
135.87	0.4045
139.07	0.4119
142.27	0.4188
145.48	0.4259
148.69	0.4333
151.91	0.4402
155.14	0.4468
158.38	0.4536
161.63	0.4608
164.90	0.4674
168.17	0.4739
171.46	0.4797
174.74	0.4863
178.04	0.4926
181.36	0.4983
184.67	0.5043

Table 1 continued

T/K	C_p/J g^{-1} K^{-1}
187.98	0.5109
191.30	0.5172
194.63	0.5231
197.97	0.5291
201.31	0.5346
204.62	0.5402
207.92	0.5454
211.19	0.5497
214.43	0.5546
217.65	0.5613
220.86	0.5661
224.06	0.5703
227.21	0.5765
230.37	0.5818
233.56	0.5855
236.70	0.5905
239.82	0.5946
242.92	0.5994
246.01	0.6040
249.08	0.6073
252.12	0.6131
255.17	0.6176
258.21	0.6203
261.22	0.6252
264.23	0.6286
267.22	0.6326
270.19	0.6380
273.17	0.6412
276.11	0.6465
279.11	0.6475
282.10	0.6517
285.02	0.6545
287.92	0.6599
290.83	0.6638
293.73	0.6671
296.63	0.6707
299.52	0.6739
302.40	0.6773
305.27	0.6805
308.14	0.6838
311.00	0.6867
313.86	0.6898
316.71	0.6937
319.59	0.6946
322.45	0.6974
Series 4	
83.78	0.2693
84.36	0.2715

Table 1 continued

T/K	C_p/J g^{-1} K^{-1}
84.88	0.2749
85.40	0.2762
85.92	0.2775
86.44	0.2800
86.96	0.2825
87.48	0.2848
88.00	0.2866
88.53	0.2884
89.05	0.2910
89.57	0.2935
90.10	0.2958
90.62	0.2980
91.15	0.3005
91.67	0.3025
92.22	0.3052
92.74	0.3075
93.27	0.3098
93.80	0.3126
94.33	0.3152
94.86	0.3190
95.39	0.3218
95.91	0.3247
96.45	0.3283
96.98	0.3321
97.51	0.3364
98.04	0.3405
98.57	0.3453
99.10	0.3508
99.63	0.3567
100.17	0.3635
100.72	0.3704
101.25	0.3748
101.78	0.3778
102.31	0.3829
102.86	0.3832
103.40	0.3578
103.95	0.3435
104.50	0.3384
105.04	0.3365
105.59	0.3357
106.13	0.3359
106.67	0.3362
107.21	0.3369
107.76	0.3383
108.30	0.3390
108.85	0.3397
109.41	0.3410
109.95	0.3423

Table 1 continued

T/K	C_p/J g^{-1} K^{-1}
110.50	0.3436
111.04	0.3448
111.59	0.3464
112.13	0.3478
112.68	0.3489
113.23	0.3501
113.78	0.3518
114.33	0.3527
114.88	0.3539
115.43	0.3551
115.98	0.3562
116.53	0.3576
117.07	0.3595
117.62	0.3607
118.20	0.3618
118.75	0.3627
119.30	0.3645
Series 5	
92.41	0.3055
92.67	0.3069
92.92	0.3084
93.17	0.3094
93.43	0.3106
93.69	0.3123
93.94	0.3141
94.20	0.3152
94.46	0.3164
94.71	0.3181
94.97	0.3196
95.23	0.3212
95.48	0.3227
95.74	0.3234
95.97	0.3255
96.25	0.3269
96.53	0.3285
96.79	0.3304
97.04	0.3321
97.30	0.3342
97.55	0.3369
97.81	0.3386
98.07	0.3406
98.32	0.3433
98.58	0.3446
98.83	0.3472
99.09	0.3499
99.34	0.3539
99.60	0.3577
99.85	0.3603

Table 1 continued

T/K	C_p/J g^{-1} K^{-1}
100.11	0.3627
100.36	0.3663
100.63	0.3685
100.88	0.3710
101.13	0.3747
101.39	0.3755
101.64	0.3765
101.89	0.3786
102.14	0.3804
102.39	0.3833
102.64	0.3868
102.90	0.3848
103.16	0.3690
103.42	0.3558
103.68	0.3476
103.94	0.3429
104.21	0.3396
104.48	0.3378
104.77	0.3372
105.04	0.3355
105.31	0.3357
105.58	0.3354
105.85	0.3351
106.12	0.3351
106.39	0.3355
106.67	0.3358
106.94	0.3361
107.21	0.3370
107.49	0.3369
107.76	0.3379
108.04	0.3388
108.31	0.3386
108.59	0.3392
108.86	0.3394
109.160	0.3405
109.44	0.3415
109.71	0.3420

[a] Points not included in the fitting

Results and discussion

In the area of 90–105 K a phase transition has been registered (Fig. 4). The authors [5, 7] pointed to the existence of the phase transition earlier based on the spectroscopic data and crystallographic investigations. Based on low-temperature relaxation microcalorimetry investigations, Geiger and Dachs [1] confirmed the availability of the phase transition at temperature of 102 K. They researched

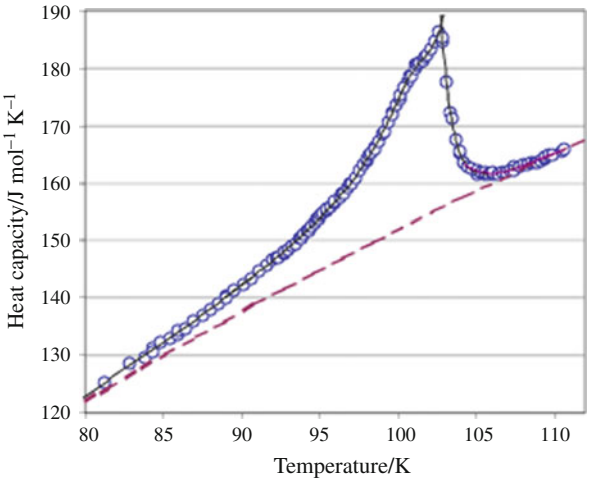

Fig. 4 The phase transition in hemimorphite

the phase transition area with the step of 1 K, and, probably, it was the reason why they did not distinguish the maximum value of the phase transition, registered by us at 102.6 K. They did not calculate changes of entropy and enthalpy of the phase transition since first of all they were interested in normal component of heat capacity, which permitted to calculate a contribution of molecular water into heat capacity of hemimorphite.

To describe the temperature dependence of heat capacity, the spline approximation of experimental values by the fifth order polynomials in the area of the phase transition and the third order polynomials over the rest range of temperatures has been used. The left and right branches of the phase transition have been processed by two polynomials in which temperature 102.8 K is the point of change of the polynomials. The intersection of the experimental points in the areas of the polynomials change was not fewer than 3–4 points and more than 5–6 points for the polynomials describing an interval of the phase transition. The values of the heat capacity polynomial coefficients in the corresponding temperature intervals are given in Table 2.

The scattering of experimental points relatively the smoothed values did not exceed ±2% at 4.5–20 K, ±0.60% at 20–80 K and ±0.27% at 120–320 K (Fig. 5). In the area of phase transition at 80–120 K, the scattering of points did not exceed ±0.70%. Extrapolation of the heat capacity values to the absolute zero was performed by means of the graphic method according to the Debye T^3 law.

It is necessary to note that in the abovementioned work of Geiger and Dachs [1] there is sufficiently big scattering between series of measurements. Thus, spread of points is about ±12% at temperature of 5 K; within the range of 25–30 K, it is about ±1%; and at temperatures of 130–300 K, it reaches the value of 0.5–0.7%.

Table 2 Hemimorphite heat capacity polynomial coefficients

Temperature interval/K	Polinomial quotients					
	A_0	a_1	a_2	a_3	a_4	a_5
5–10	-6.6578×10^{-2}	5.9719×10^{-2}	-1.8626×10^{-2}	2.9493×10^{-3}		
10–20	3.9012	−1.1360	1.0361×10^{-1}	-1.2863×10^{-3}		
20–40	−5.9415	2.3424×10^{-1}	4.0029×10^{-2}	-3.0064×10^{-4}		
40–70	-3.2903×10^{1}	2.0622	-2.2474×10^{-4}	-1.5502×10^{-5}		
70–90	-2.3796×10^{2}	1.0388×10^{1}	-1.1313×10^{-1}	4.9612×10^{-4}		
90–100	-1.1207×10^{6}	6.0421×10^{4}	-1.3031×10^{3}	1.4055×10^{1}	-7.5813×10^{-2}	1.6362×10^{-4}
100–102.8	9.4415×10^{8}	-4.6273×10^{7}	9.0700×10^{5}	-8.8876×10^{3}	4.3538×10^{1}	-8.5297×10^{-2}
102.8–106	5.5876×10^{8}	-2.6213×10^{7}	4.9187×10^{5}	-4.6146×10^{3}	2.1646×10^{1}	-4.0611×10^{-2}
106–110	6.5648×10^{4}	-1.8086×10^{3}	1.6640×10^{1}	-5.1000×10^{-2}		
110–120	-4.8752×10^{2}	1.5257×10^{1}	-1.2584×10^{-1}	3.7338×10^{-4}		
120–180	−9.6965	1.9200	-3.2422×10^{-3}	1.3971×10^{-6}		
180–240	-6.1258×10^{1}	2.7402	-7.6924×10^{-3}	9.6533×10^{-6}		
240–320	2.3148×10^{2}	-7.3620×10^{-1}	6.1699×10^{-3}	-8.9267×10^{-6}		

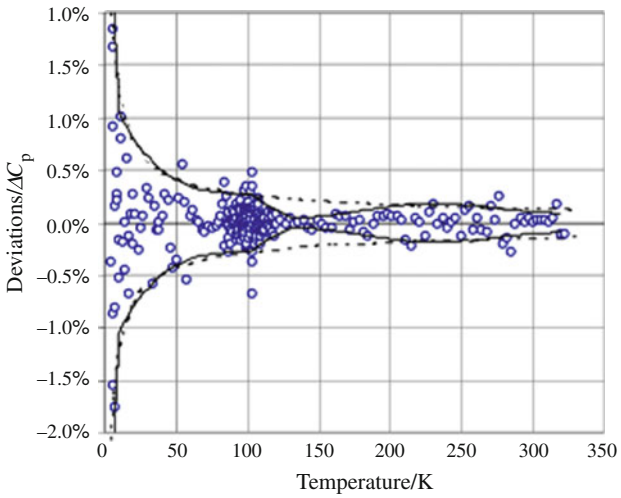

Fig. 5 Deviations of the hemimorphite heat capacity experimental values from smoothing polynomial

The tabulated values C_p, S_T, and $H_T - H_0$ of hemimorphite have been calculated based on the obtained coefficients of polynomials. The values of thermodynamic functions of hemimorphite (taking the phase transition contribution into account) are given in Table 3. A relative error of the obtained values was determined from deviations of the experimental data from the smoothed ones by two ways: through the corridor of deviations by means of the power function (a dotted line in Fig. 5) and by more detailed description of the spread in values by the set of third order polynomials (a firm line in Fig. 5). In the first case the relative error for the heat capacity is ±0.14%, for entropy ±0.26%, and for enthalpy ±0.20%; in the second case, these values are ±0.11%, ±0.21% and ±0.16%, respectively. It should be noted that normally a measurement error of the heat capacity at the given unit does not exceed ±0.10% over the range of 100 K in the absence of the phase transition.

It should be noted that the errors of standard values of the heat capacity and entropy given in the work of Geiger and Dachs [1] exceed those obtained by us by the order of magnitude.

To determine the thermodynamic characteristics of the phase transition in hemimorphite the heat capacity component has been calculated without taking an anomalous contribution into consideration. The set of the experimental values from series 2 and 3 over the interval 37.9–155.2 K, except the points from 81.26 to 107.47 K inclusive, has bee subjected to smoothing by the third order polynomial. The obtained coefficients are equal to: $a_0 = -29.05878$, $a_1 = 2.28815$, $a_2 = -5.58852 \times 10^{-3}$, $a_3 = 6.40608 \times 10^{-6}$. The intersection interval of the heat capacity anomalous dependence with the obtained polynomial, in which the phase transition was calculated, was 70–110 K. The maximal experimentally registered point of the phase transition is at 102.644 K and 186.33 J mole^{-1} K^{-1}; however, two branches of the phase transition, which this or that point belongs to, can be clearly distinguished on the plot. The intersection of the polynomials, describing these branches, in the point of the phase transition is at temperature 102.8 K with heat capacity 187.73 J mole^{-1} K^{-1}, and the change of polynomials occurred at this value when calculating the thermodynamic functions. The entropy and enthalpy of the phase transition obtained by the difference of values of the anomalous heat capacity and the obtained polynomial are $\Delta S = 2.410 \pm 0.063$ J mole^{-1} K^{-1} and $\Delta H = 234.17 \pm 5.71$ J mole^{-1}. The values of changing of the phase transition entropy and

Table 3 Thermodynamic functions of hemimorphite ($M_r = 481.757$ g mole^{-1})

T/K	C_p/J mole^{-1} K^{-1}	S_T/J mole^{-1} K^{-1}	$H_T - H_0$/J mole^{-1}
5	0.135	0.038	0.147
10	1.617	0.452	3.534
15	5.833	1.811	21.00
20	12.34	4.337	65.68
25	20.24	7.921	146.73
30	28.99	12.37	269.48
35	38.40	17.54	437.75
40	48.23	23.31	654.22
45	58.03	29.56	919.92
50	67.71	36.17	1234.3
55	77.26	43.07	1596.8
60	86.67	50.20	2006.7
65	95.93	57.51	2463.3
70	105.0	64.95	2965.8
75	114.1	72.50	3513.6
80	123.0	80.15	4106.3
85	132.3	87.89	4744.4
90	142.3	95.73	5430.5
95	153.9	103.7	6169.3
100	174.2	112.0	6982.3
102.8	187.7	117.0	7488.4
105	161.9	120.6	7859.5
110	165.1	128.2	8673.4
120	176.4	143.0	10380
130	188.2	157.6	12204
140	199.4	172.0	14142
150	210.1	186.1	16190
160	220.2	200.0	18342
170	229.9	213.6	20593
180	239.0	227.0	22938
190	247.9	240.2	25373
200	256.3	253.1	27894
210	264.3	265.8	30498
220	272.1	278.3	33180
230	279.5	290.6	35938
240	286.8	302.6	38770
250	293.6	314.5	41671
260	300.3	326.1	44641
270	306.8	337.6	47676
273.15	308.8	341.1	48646
280	313.1	348.8	50776
290	319.2	359.9	53937
298.15	323.9 ± 0.3	368.8 ± 0.5	56558 ± 51
300	324.9	370.8	57158
310	330.3	381.6	60434
320	335.2	392.1	63761

enthalpy obtained by the graphic method are $\Delta S = 2.52 \pm 0.01$ J mole^{-1} K^{-1} and $\Delta H = 249 \pm 0.3$ J mole^{-1}.

The line of the heat capacity temperature dependence of hemimorphite at the phase transition has a peculiar shape differing from the usual λ-shape. It allows to assume that the phase transition itself over a comparatively narrow temperature interval is a complex process. In their work, Libowitzky et al. [7] show that a low-temperature modification of hemimorphite crystal structure below the point of phase transition is characterized by the turn of water molecules and reorientation of hydroxyl groups in the plane of crystallographic vectors a–c. It should be noted that according to the experimental measurement results, we have not detected any traces of the influence of the phase transition detected by Kolesov using the spectroscopic methods on the heat capacity temperature dependence of hemimorphite in the area of temperatures about 20 K.

Calculation of vibrational and thermodynamic properties of hemimorphite

The current methods of analysis of solids allow to calculate thermodynamic functions of compounds on the basis of data on a substance crystal structure taking into account its vibrational states. Calculation of the temperature dependence of hemimorphite heat capacity has been made based on the given methods. Program LADY (LAttice DYnamics toolkit) [11] has been used for calculations. This program permits to compute vibrational properties of solids in the framework of the theory of crystal lattice dynamics. The atomic coordinates of high-temperature modification of hemimorphite from the work [3] were used when computing. Calculation of vibrational states was made according to a valence force field model; for this purpose a

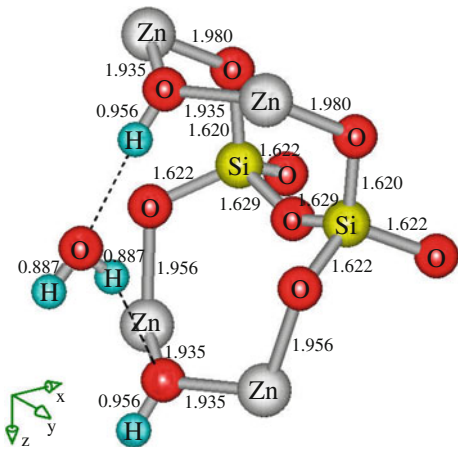

Fig. 6 Molecular fragment in crystal structure of hemimorphite and valence bonds lengths, Å

Table 4 Experimental and calculated vibrational spectra of hemimorphite

Raman spectrum		Infrared spectrum	
ν_{calc}/cm^{-1}	ν_{exp}/cm^{-1} [8]	ν_{calc}/cm^{-1}	ν_{exp}/cm^{-1} [8]
97		117	
117	111	120	
120		140	
132	132	143	
140		146	
143		157	
146		200	
157	157	202	
160	168	208	
180		213	
200	193	226	
202		232	
208		242	
213	213	247	
226		247	
232	230	283	
232		301	
242		303	
247		329	
247		360	
283	274	374	
301		408	
302		424	
303		483	
329	330	491	
360		517	
374		527	
408	399	570	
424		573	597
483	451	605	609
491			676
492			702
517			709
527		751	737
537		801	831
570	555	829	836
573		913	863
575		926	894
605		931	933
	674	970	974
751		978	1027
801			1043
829			1049
913		1079	1078
921		1147	1105
926	926		1335
931	930		1336
970			1357
978	996		1386
1079			1496
1079			1514
1147	1180		1548
	1366		1588
1646	1634	1646	1633
3185	3240	3185	3180
3186	3321	3186	3234
3405	3455	3405	3297
3491	3565	3491	3352

set of force constants of valence bonds and angles was determined based on the computed hemimorphite crystal structure (Fig. 6). Calculation of initial values of the compound force constants was made by the semi-empirical method of quantum chemical calculations PM5. The calculated values of force constants were used when calculating vibrational states of the crystal lattice and modeling the IR and Raman spectra of hemimorphite in LADY program. As a validation criterion of the calculations, the agreement of the design and experimental spectra of hemimorphite borrowed from work [8] in which individual components of the band of experimental IR and Raman spectra had been determined were used. For this purpose, a procedure of sequential variation of the initial force constants values was performed, as a result of which a satisfactory fit of the design lines positions in the theoretical spectrum and those of absorption bands in the experimental spectra (Table 4) was reached. On the basis of the obtained set of hemimorphite vibrational states, the calculation of the compound background states was made, and its thermodynamic functions, heat capacity and entropy were calculated over the temperature range 10–300 K.

The computation of hemimorphite thermodynamic functions was also made by the semi-empirical method of quantum chemical calculations PM5 using program MOPAC permitting to make calculations for the extended structures. The calculation was made on an atomic cluster consisting of two unit cells of the mineral; thus, 80 atoms took part in the calculation, and lateral dimensions of the cluster were 8.37 × 10.73 × 10.23 Å. The Born-von Karman boundary conditions were used while calculating, and that provided the correctness of the performed quantum chemical calculation of structural and thermodynamic properties of the compound.

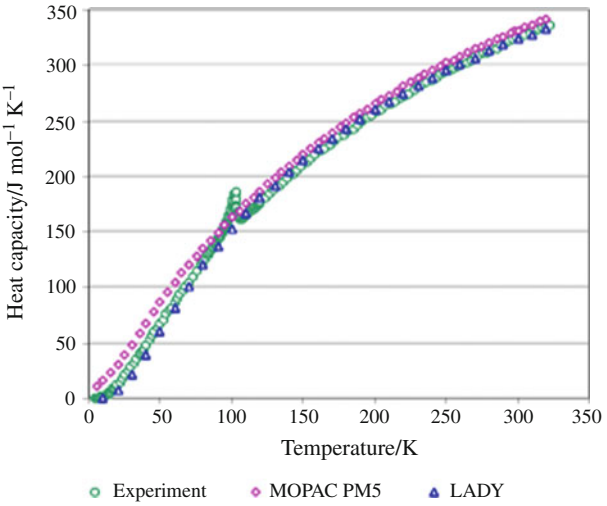

Fig. 7 Experimental and calculated temperature dependencies of hemimorphite heat capacity

As a result of quantum chemical computation over the temperature range 10–300 K, the magnitude of the following thermodynamic values of the mineral were obtained: heat capacity, enthalpy and heat of formation. The magnitude of design values of molar heat capacity of the compound at standard temperature was 329.9 J mole^{-1} K^{-1} (computation made by MOPAC) and 321.7 J mole^{-1} K^{-1} (computation made by LADY). The analysis of the values obtained and their correlation with the experimental data (Fig. 7) show that the calculated values correlate satisfactorily with the experiment, particularly in the range of temperatures higher than the phase transition. The values of heat capacity calculated according to the found vibrational states agree satisfactorily with the experimentally obtained data to within ±1.7% over the range of 120–200 K, and not more than ±0.8% for the range of 200–300 K.

Conclusions

Thus, the experimental values of thermodynamic functions of a natural silicate of zinc hemimorphite have been obtained as a result of the carried out investigations. These values have been confirmed by the calculation methods.

References

1. Geiger CA, Dachs E. Quasi-ice-like C_p behavior of molecular H_2O in hemimorphite $Zn_4Si_2O_7(OH)_2 \bullet H_2O$: C_p and entropy of confined H_2O in microporous silicates. Am Mineral. 2009;94:634–7.
2. McDonald WS, Cruickshank DWJ. Refinement of the structure of hemimorphite. Z Krist. 1967;124:180–91.
3. Hill RJ, Gibbs GV, Craig JR, Ross FK, Williams JM. A neutron-diffraction study of hemimorphite. Z Krist. 1977;146:241–59.
4. Takeuchi Y, Sasaki S, Joswig W, Fuess H. X-ray and neutron diffraction study of hemimorphite. Proc Jpn Acad. 1978;B54:577–82.
5. Libowitzky E, Rossman GR. IR spectroscopy of hemimorphite between 82 and 373 K and optical evidence for a low-temperature phase transition. Eur J Mineral. 1997;9:793–802.
6. Libowitzky E, Kohler T, Armbruster T, Rossman GR. Proton disorder in dehydrated hemimorphite-IR spectroscopy and X-ray structure refinement at low and ambient temperatures. Eur J Mineral. 1997;9:803–10.
7. Libowitzky E, Schultz AJ, Young DM. The low-temperature structure and phase transition of hemimorphite, $Zn_4Si_2O_7(OH)_2 \cdot H_2O$. Z Krist. 1998;213:659–68.
8. Frost RLW, Bouzaid JM, Reddy BJ. Vibrational spectroscopy of the sorosilicate mineral hemimorphite. Polyhedron. 2007;26:2405–12.
9. Kolesov B. Raman investigation of H_2O molecule and hydroxyl groups in the channels of hemimorphite. Am Mineral. 2006;91:1355–62.
10. http://www.termax.ru. Accessed July 2010.
11. Smirnov M, Kazimirov V. LADY: software for lattice dynamics simulations. Dubna: Communication of the Joint Institute for Nuclear Research; 2001.